Aalborg Universitet

AALBORG UNIVERSITY
DENMARK

Line Differential Protection Scheme Modelling for Underground 420 kV Cable Systems

Sztykiel, Michal; Bak, Claus Leth; Dollerup, Sebastian

Published in:
Journal of Energy and Power Engineering

Publication date:
2011

Document Version
Publisher's PDF, also known as Version of record

Link to publication from Aalborg University

Citation for published version (APA):
Sztykiel, M., Bak, C. L., & Dollerup, S. (2011). Line Differential Protection Scheme Modelling for Underground 420 kV Cable Systems. *Journal of Energy and Power Engineering*, 799-808.

General rights
Copyright and moral rights for the publications made accessible in the public portal are retained by the authors and/or other copyright owners and it is a condition of accessing publications that users recognise and abide by the legal requirements associated with these rights.

- Users may download and print one copy of any publication from the public portal for the purpose of private study or research.
- You may not further distribute the material or use it for any profit-making activity or commercial gain
- You may freely distribute the URL identifying the publication in the public portal -

Take down policy
If you believe that this document breaches copyright please contact us at vbn@aub.aau.dk providing details, and we will remove access to the work immediately and investigate your claim.

Downloaded from vbn.aau.dk on: April 09, 2024

Journal of Energy and Power Engineering 6 (2012) 799-808

Line Differential Protection Scheme Modelling for Underground 420 kV Cable Systems

Michal Sztykiel[1], Claus Leth Bak[1] and Sebastian Dollerup[2]

1. Department of Energy Technology, Aalborg University, Aalborg DK-9220, Denmark

2. Transmission Line Department, Energinet.dk, Fredericia DK-7000, Denmark

Received: March 17, 2011 / Accepted: August 31, 2011 / Published: May 31, 2012.

Abstract: Based on the analysis of a specific relay model and an HVAC (high voltage alternating current) cable system, a detailed approach to EMTDC/PSCAD modelling of protective relays is presented. Such approach allows to create complex and accurate relay models derived from the original algorithms. Relay models can be applied with various systems, allowing to obtain the most optimal configuration of the protective relaying. The present paper describes modelling methodology on the basis of Siemens SIPROTEC 4 7SD522/610. Relay model was verified experimentally with its real equivalent by both EMTP-simulated and real world generated current signals connected to the relay.

Key words: Line differential protection, XLPE HVAC cable, EMTDC/PSCAD relay model, SIPROTEC 4 7SD522, 7SD610.

1. Introduction

Relay computer modelling is an important issue for establishing proper protection scheme over the specified system. Role of the relay models for power systems has been already discussed in Refs. [1, 2]. References provide general modelling approach and present problems related to the development of good relay models.

Nowadays, it is difficult to obtain accurate relay computer model, since relay manufacturers offer their products with a variety of algorithms and features that may significantly change operation of relays under specific conditions and states.

Generic relay models based on general design concepts have been widely introduced in Refs. [3-6]. These models provide sufficient accuracy for investigating and studying many protection-related problems. However, they lack accuracy for optimal relay programming, which becomes crucial and most desired for industrial applications.

For this purpose, essential study over detailed approach for creating relay models in EMTDC/PSCAD is given. The methodology relies on obtained relay's technical specification (given by relays manufacturer), so that unique features and algorithms-characteristic for each relay type can be developed.

As a result, this would give complex relay model narrowed and useful only for specified type of relay. In compensation, relay computer model would be very accurate (mainly in terms of sensitivity and operating speed) with easy and user-friendly configuration panel, which is programmed with the same parameter values as in real devices.

Established relay models would easily allow to perform simulations of chosen study cases and examine possibilities of unwanted tripping that might occur (e.g. due to transient power electronics switching, overvoltages, external faults, energization states, etc.).

This paper presents such analysis for Siemens line differential relays SIPROTEC 4 SD522/610, as these relays are planned to protect HVAC underground

Corresponding author: Claus Leth Bak, professor, M.Sc., research fields: power system transients, transmission cable systems, protection and HVDC-VSC. E-mail: clb@et.aau.dk.

transmission cable system built in Denmark in years 2012-2014.

Large capacitance of underground cables in comparison to overhead lines brings original issues for the differential protection scheme to consider, as both steady and transient states have to be deeply analyzed. For steady state, charging current is the factor that mostly affects relays function. For transient states, relays may be affected by inrush currents that occur due to shunt reactors switching operations (necessary for reactive power compensation).

In order to properly reflect cable system's influence over relay's current signals in mentioned states, cable system is modelled with the usage of EMTDC/PSCAD software, as it provides satisfactory accuracy for both steady and transient analysis.

When both cable system and protection scheme models are completed, relay model's accuracy can be finally verified through experimental testing. Having identical parameter setting both for relay model and real device, sensitivity and operating speed are compared thus showing high accuracy of the relay model.

Results from experimental analysis prove that presented approach for relay modelling can be successfully adapted for specific relays with original algorithms and features.

2. Protected Cable System Background

2.1 Description of Cable System

The single phase diagram of total cable system is shown in Fig. 1.

The system consists of the following components:

(1) XLPE HVAC underground cable sections (L1-L2): Selected cable is made of three aluminium single-core cables buried underground on the depth of 1.3 m and laid in a flat formation within 300 mm from each other. Total cable is divided into two sections of lengths accordingly 28 km and 29.5 km. Metallic screens of each cable section are cross-bonded approximately each 2 km, and earthed each 6 km. Detailed information about cable structure is presented in Table 1.

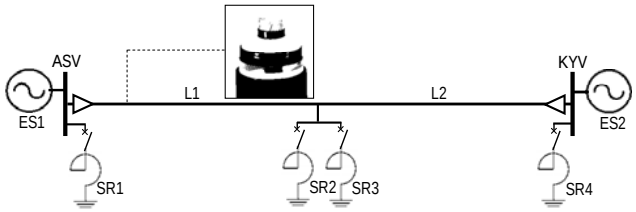

Fig. 1 Schematic representation of the underground 420 kV cable system.

Table 1 Technical data of XLPE underground 420 kV cable.

Description	Value
Cross-section of conductor (mm^2)	1,600
Diameter of conductor (mm)	52
Insulation thickness (mm)	27.0
Diameter over insulation (mm)	110.0
Cross-section of screen (mm^2)	185
Outer diameter of cable (mm)	127.0
Capacitance (μF/km)	0.21
Inductance (mH/km)	0.50
Charging current per phase (A/km)	14.9

(2) Shunt reactor banks (SR1-SR4): Four switchable shunt reactors are used for the reactive power compensation. First two are rated for 100 MVARs and located in the ASV and KYV stations, while the other two rated for 140 MVARs are installed in the middle of the cable system, thus interconnecting adjacent cable sections.

(3) Supply sources (ES1-ES2): Power system on both sides of the cable is modelled by ES1 and ES2 sources that are Thevenin equivalents consisting of voltage sources and its short-circuit impedances. Parameter values are listed in Table 2.

2.2 EMTDC/PSCAD Model of Cable System

In Fig. 2, described cable system is modelled in EMTDC/PSCAD software by frequency dependent (phase) model, giving highest accuracy among other available models [7]. Such modelled cable system may accurately reflect the behaviour of the protection scheme under various transient states that are likely to appear. Further detailed information about establishing computer model of the cable is available in Ref. [7].

Shunt reactors are modelled with series resistance and inductance parameter values for each phase.

Table 2 Technical data of cable's supply sources.

Supply source	Voltage (kV)	Short-circuit impedance (Ω)
ES1	420	0.829 + j16.60
ES2	420	0.839 + j16.78

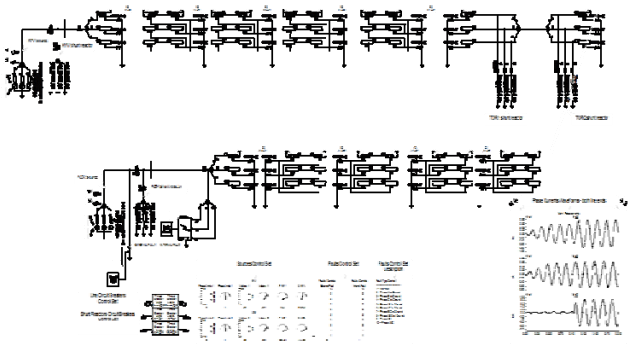

Fig. 2 EMTDC/PSCAD representation of the underground 420 kV cable system, where KYV, TOR and ASV are respectively Kyndbyværket, Torslund and Asnæsværket substations located on the Zealand island in Denmark.

Table 3 shows validation results for three possible currents that can flow through protected cable. Parameters were chosen that mostly affect proper function of established differential protection. Detailed methodology for cable model validation along with series of calculations is given in Refs. [7-9].

Relative error originates from cable geometry, since mutual couplings between internal conductive cable layers take place. This corresponds to core conductors and screens that are in close proximity to each other. Resulting inductive reactance for single phase is lower than calculated algebraically, thus giving higher current value which rises significantly when high currents flow through cable [8].

Validation results allow to conclude that certain error level occurs and has to be taken into account. Higher fault current values from EMTDC/PSCAD simulations allow to keep safety margin for the analysis based on simulation results.

2.3 Description of Differential Protection Scheme

Total differential protection scheme for the analyzed cable system is presented in Fig. 3.

Proposed protection scheme consists of following components:

Table 3 Validation results for EMTDC/PSCAD underground cable model.

Description	Theoretical analysis	EMTDC/PSCAD model	Relative error e_r (%)
Maximum charging current (kA)	0.878	0.805	8.3
External fault at ASV substation (kA)	9.555	11.49	16
Internal fault in the middle of the cable (kA)	11.85	12.94	8.4

Relative error e_r is calculated from the formula $e_r = \frac{100 \cdot |I_{TA} - I_{PSCAD}|}{I_{TA}}$, where I_{TA} is the current parameter value obtained algebraically and I_{PSCAD} is the current parameter value obtained numerically.

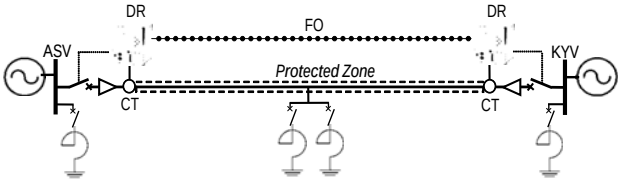

Fig. 3 Schematic representation of the differential protection scheme over underground 420 kV cable system, where DR means differential relay, FO is fibre optic cable and CT is current transformer.

(1) CT (current transformers): Devices responsible for current signal transformation on the level applicable for measuring instruments installed in protection relays. Table 4 shows current transformers specification used for computer modelling purpose.

(2) Mono-mode FO (fibre optic cables): Communication channels responsible for proper signal transmission between relays. Due to significant length of the protected cable (58.5 km), signal attenuation phenomenon must be considered along with time delay between sending and reaching signal from both sides of the protected cable. Ref. [8] explains detailed solution methodology to stated issues. Channel time delay is calculated based on datasheet provided by fibre optic cable's and relay's manufacturers. Necessary data are gathered in Table 5.

Channel time delay T_{delay} is 1.07 ms, calculated from

$$T_{delay} = T_s + T_t + T_r = \frac{l_B}{v_B} + \frac{l_{FO}}{v_{FO}} + \frac{l_B}{v_B}. \quad (1)$$

where

T_s—time for sending signal by the local relay;

T_t—time for transmitting signal through FO cable;

T_r—time for receiving signal by the remote relay.

Table 4 Technical data of CT (current transformers).

Parameter	Value
CT manufacturer's model	ABB IMB 420
CT class	5P
Transfomation ratio (A/A)	1000/1
Accuracy Limit Factor ALF	100
Nominal power (VA)	15

Table 5 Technical data of FO (fibre optic cables).

Index	Parameter	Value
v_B	Bandwidth data speed (bits/s)	512
l_{FO}	FO length (km)	58.5
v_{FO}	FO speed of light (km/s)	200,000
l_B	HDLC frame length (bits)	200

(3) Line DR (differential relays): Most complex components realizing signal measurement, signal comparison and finally—fault detection principles. Relays analyzed in this paper are Siemens SIPROTEC 4 7SD522. Detailed technical specification, instruction on establishing proper configuration parameter set are available in Refs. [7-9].

2.4 EMTDC/PSCAD Model of Differential Protection Scheme

A general approach is introduced for protection scheme modelling in PSCAD software.

Based on previous components description, their unique characteristic functions are presented below. Each component is responsible for:

- Signal transformation, modelled by current transformer Lucas model blocks with specified parameter settings. Ref. [10] provides more information regarding CT Lucas model;
- Signal transmission, modelled by time delay blocks with specified and calculated time delay value from Eq. (1);
- Signal processing, modelled with complex block combination, reflecting operation algorithm and original features of real relays.

3. EMTDC/PSCAD Relay Modelling

Relay EMTDC/PSCAD computer model is created in a shape of box with three phase modules included, so that all operations are phase segregated as in real relays. Input signals for modules are previously sampled with sampler blocks, so that 20 sampled values appear each full cycle period (fixed frequency) [8].

Output logic signal *B1* is responsible for controlling line circuit breaker in case of possible fault occurrence. Following features are included in each phase module:

(1) Sample acquisition: Operation necessary for further phasor and charge computations. Sample values i_n have to be stored during full cycle. This operation is available by implementing 20 Sample/Hold blocks—each controlled by logic pulse generator block, as presented in Fig. 4. Pulse generator blocks give command D for each sample/hold block. Generated pulses are shifted to each other by 18 degrees of total cycle period.

(2) Phasor measurement: Current phasor values *I* are obtained in the shape of complex numbers through discrete Fourier transform technique, based on

$$\underline{I} = I_S + j \cdot I_C. \tag{2}$$

where

$$I_S = \frac{2}{N} \cdot \left[\sum_{n=1}^{N-1} sin(\omega \cdot n \cdot \Delta t) \cdot i_n \right]. \tag{3}$$

$$I_C = \frac{2}{N} \cdot \left[\frac{i_0}{2} + \frac{i_N}{2} + \sum_{n=1}^{N-1} cos(\omega \cdot n \cdot \Delta t) \cdot i_n \right] \tag{4}$$

Here there are:

n = 1, 2,…, 20—sample number;

i_n—current sample value corresponding to sample n;

$\omega = 2 \cdot f \cdot \pi$—cycle pulsation;

$\Delta t = (f \cdot N)^{-1}$—sample time interval;

f = 50 Hz—frequency;

N = 20—number of samples over one cycle.

Eqs. (3) and (4) are realized by correlating sample values with sine and cosine waveforms and summating them each full cycle period [7].

(3) Charge measurement: Charge values *Q* are obtained based on

$$Q = \int_{0+n}^{5+n} i \cdot dt \approx \sum_{i=n}^{n+5} i_i \cdot \Delta \tilde{t}_i \tag{5}$$

Four charge values are calculated each full cycle period. By applying signal switch block, final charge

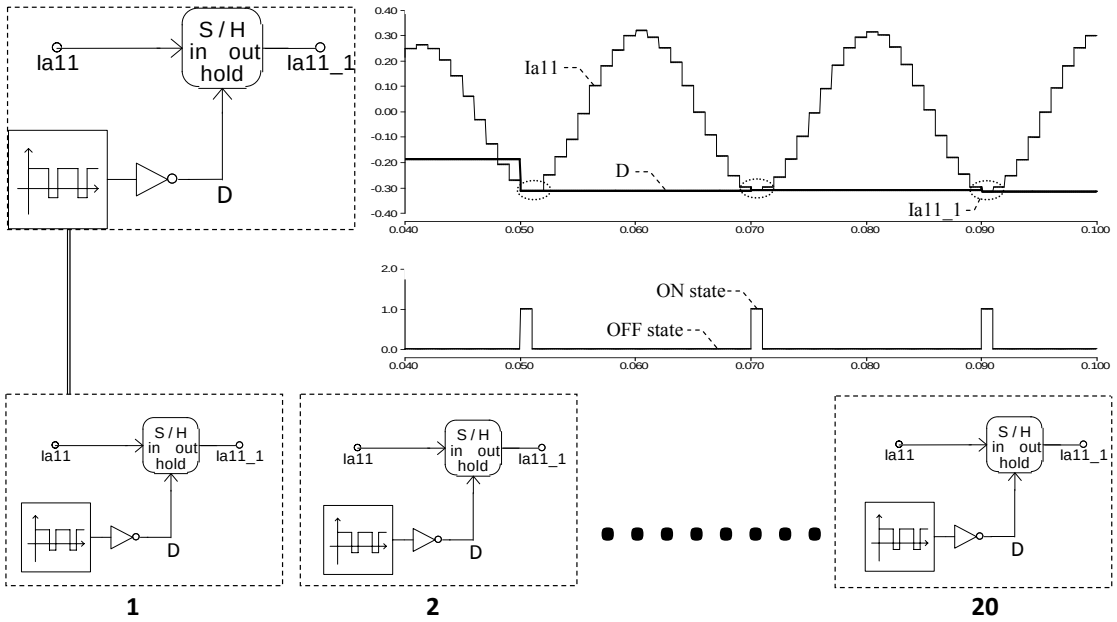

Fig. 4 EMTDC/PSCAD representation of sample acquisition technique.

signal is switched each quarter cycle. This corresponds to real relay feature, where charge comparison is performed four times more often than phasor comparison.

(4) Phasor comparison: Based on relay's principles given in Ref. [1], values for operational phasor I_{OP} and restraint phasor I_{RES} are obtained and relay operating criterion is

$$I_{OP} > I_{RES} \tag{6}$$

for

$$I_{RES} = I_{diff>} + \begin{cases} P2 \cdot |\underline{I}_1| : & |\underline{I}_1| \leqslant P1 \\ P3 \cdot |\underline{I}_1| : & |\underline{I}_1| > P1 \end{cases} + \begin{cases} P2 \cdot |\underline{I}_2| : & |\underline{I}_2| \leqslant P1 \\ P3 \cdot |\underline{I}_2| : & |\underline{I}_2| > P1 \end{cases} \tag{7}$$

$$I_{OP} = \left| \underline{I}_1 + \underline{I}_2 \right| \tag{8}$$

Relay setting parameters *P1*, *P2*, *P3* and $I_{diff>}$ are chosen based on procedure given in Refs. [9, 10]. Parameters I_1 and I_2 are current phasor values correspondingly measured by local and remote relays. Operation of switching multiplying factors for restraint phasor (determined by current signal value—in fault state or load state) is made with the usage of comparator blocks, which output signal is multiplied by its corresponding actual phasor current signal value, as shown in Fig. 5.

Based on information obtained from the position of line circuit breaker installed on the same side as device, differential relay can detect "dead line" state when no current flows through the protected cable. Cable energization state—when circuit breaker is suddenly switched on that is detected by Edge Detector block by positive transition appearance of signal from line circuit breakers. This allows generating digital impulse, which is later extended to the specified time interval—*Td* setting, which can be changed based on relay settings by Monostable Multivibrator block.

(5) Charge comparison: For this technique, the same algorithm is used as for phasor comparison. $I_{diff>}$ parameter is replaced with minimum threshold value for charges: $I_{diff>>}$. In addition, phasor signals are replaced with their corresponding operational Q_{OP} and restraint Q_{RES} charge values.

(6) Signal filtering: Operational and restraint values are filtered using low-pass Butterworth filter block with established frequency threshold corresponding to each comparison technique.

(7) Inrush restraint: 2nd harmonic phasor currents $\underline{I}_{2nd}$ are measured by online frequency scanner blocks. If its values exceed established ratio k_{ratio} of 1st

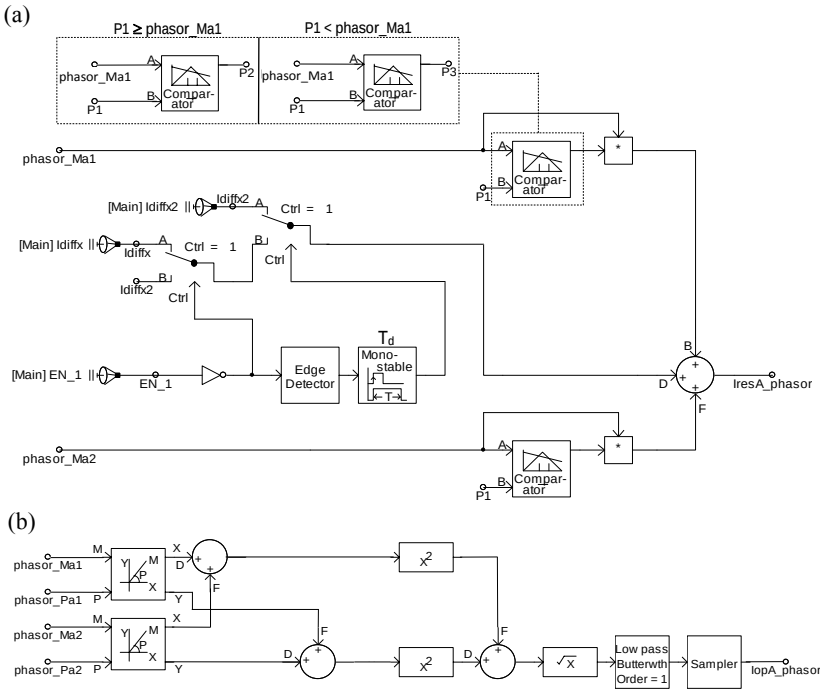

Fig. 5 EMTDC/PSCAD representation of phasor comparison technique: (a) restraint phasor *IresA_phasor* and (b) operational phasor *IopA_phasor* are final signals. Derived phasor magnitude signals *phasor_Ma1* and *phasor_Ma2* are used as input variables along with associated phase values *phasor_Pa1* and *phasor_Pa2*. Input constants set by the user are relay differential arbitrary threshold values: *Idiffx* and *Idiffx2* during energization state. *P1* is set as a relative threshold signal for varying multiplying factor from *P2* to *P3*. Finally, EN_1 is an external signal that provides information on the switching position of the line breaker, so that "dead line" state can be detected.

harmonic $\underline{I}_{1st}$, relay prevents tripping operation. In EMTDC/PSCAD model this feature can be switched OFF as in real relays. Condition statement (9) has to be fulfilled in order to activate inrush restraint blocking feature. Upper limit for non-tripping operation is established with I_{max_peak} parameter

$$\left(\left|\underline{I}_{2nd}\right| > k_{ratio} \cdot \left|\underline{I}_{1st}\right|\right) \wedge \left(\left|\underline{I}_{1st}\right| < I_{max\_peak}\right) \quad (9)$$

Comparison principles are obtained with a combination of comparator blocks. Output signals from comparators can then be combined with logic gates so that tripping signal depends on the resulting signal from the inrush restraint feature.

(8) Cross-blocking: In order to prevent tripping signals from all three phases when inrush feature is active in only single phase, cross-blocking feature is introduced. Its PSCAD representation is shown in Fig. 6.

In EMTDC/PSCAD computer model, cross-blocking utilizes single phase tripping and inrush activation signals as the output signals of each phase module. Combining them all with logic gates gives final tripping signal decision *B1*. Hence, described feature has to be implemented outside phase modules. As in real relays, feature can be permanently switched OFF during normal operation.[1]

4. EMTDC/PSCAD Simulation Cases

4.1 Two-Phase External Fault at KYV Substation

External fault simulation in phases A and B allows analysis on how relay computer model reacts when high currents flow through the protected cable. Fault is cleared after 55 ms by virtual bus protection installed in place where fault occurred. All shunt reactors are disconnected (highest charging current). Simulation graphs are presented in Fig. 7.

[1] Original EMTDC/PSCAD files with fully established and configured models of the relays and protected cable system are available at main author on request.

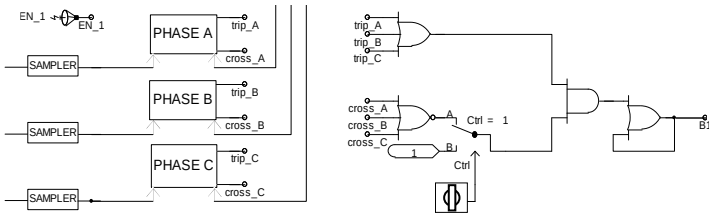

Fig. 6 EMTDC/PSCAD representation of cross-blocking technique.

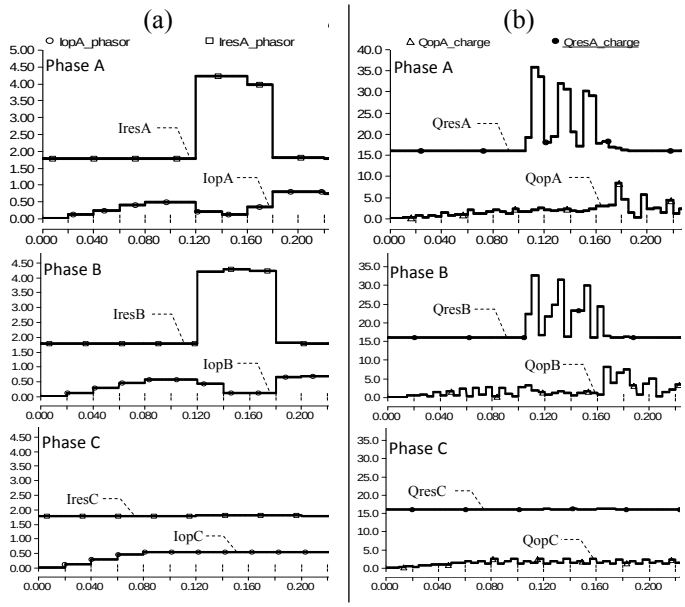

Fig. 7 External fault state at 10 ms. (a) Operational phasors *Iop* are compared with restrained phasors *Ires* through phasor comparison technique for each phase; (b) Operational charges *Qop* are compared with restraint charges *Qres* through charge comparison technique for each phase.

Due to high currents flowing through phases A and B which are higher than calculated *P1* value [9], transition takes place resulting in switching multiplying factors from *P2* to *P3* value. This means that transformed secondary current lies within fault area and security margin is increased in corresponding phases.

On presented plots, restraint threshold *Ires* and *Qres* are higher for the time when external fault current flows. After fault clearing, restraint values return to their normal threshold levels since transformed current lies once again within load area. An increase of operational values *Iop* and *Qop* in phases with high current appears after fault clearing, giving large safety margin in order to prevent unwanted tripping. It is seen that during whole simulation operational values do not exceed restraint ones. As a result, relay properly does not detect any fault within protected cable and does not send tripping signal.

4.2 Single-Phase Intenal Fault at KYV Substation

Simulation test involves internal fault appearance in phase A within protected cable. As the worst case scenario, single A-phase fault is applied with high resistance R_{fault} = 20 Ω and all shunt reactors are switched ON (lowest charging current). Computer model with established setting parameters should be able to properly detect and recognize fault state within phases. Fig. 8 presents described simulation case results.

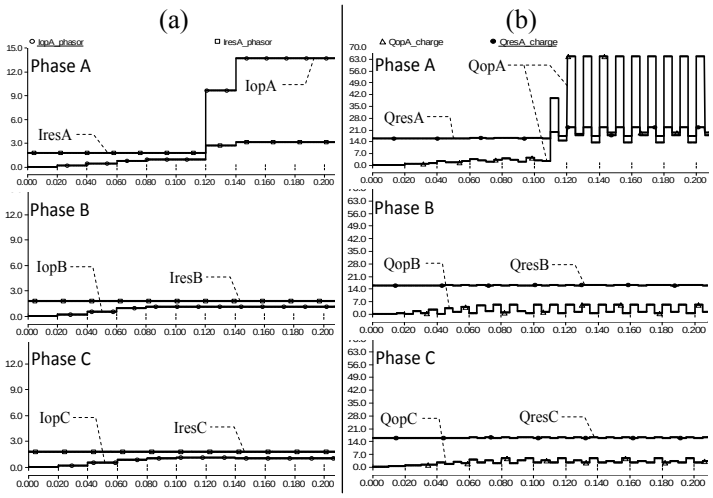

Fig. 8 Internal fault state at 10 ms. (a) Operational phasors *Iop* are compared with restrained phasors *Ires* through phasor comparison technique for each phase; (b) Operational charges *Qop* are compared with restraint charges *Qres* through charge comparison technique for each phase.

As expected, internal fault occurred in A phase and is detected by relay computer model both with phasor and charge comparison techniques. Operational values *Iop* and *Qop* significantly exceed restraint ones after 20 ms from fault occurrence for phasor and 15 ms for charge comparison principles. Earlier fault detection with charge technique results in sending tripping signal after 15 ms in order to disconnect faulted cable.

5. Relay Testing

5.1 Description

Relay experimental testing is possible with the usage of modern equipment and software capable of converting current signals from EMTDC/PSCAD software into current waveforms injected into real differential relays. Simplified diagram of experimental test setup is presented in Fig. 9.

Six current signals are sent: *Ia11*, *Ib11*, *Ic11*, *Ia22*, *Ib22*, *Ic22* from which three enter to each relay accordingly to the side from which they were measured. Interconnected relays via fibre optic cable respond based on delivered signals with measured values and annunciation messages saved as logs.

These logs can then be sent to PC and read in DIGSI software for further analysis and for comparison purposes.

5.2 Results

All tests from experimental analysis and EMTDC/PSCAD simulations were performed with the same setting parameter values. Relay's operating speed and sensitivity have been examined.

(1) Operating speed: Operating speed analysis gives idea on how fast relay is able to detect fault states. By the analysis of restraint/operational plots in EMTDC/PSCAD computer software, time interval between exceeding threshold by operational charge value Q_{OP} and phasor value I_{OP} can be compared with the ones obtained from DIGSI logs. Analyzed study case results are presented in Table 6.

(2) Sensitivity: Relay's sensitivity analysis is critical for proper internal fault states recognition. For this reason, internal faults with very high resistance values were analyzed. Differential threshold parameter $I_{diff>}$ for phasor comparison was adjusted in order to obtain its critical threshold values. Results are listed and compared in Table 7. Phasor comparison is examined since it is more sensitive and necessary for proper fault detection. Critical values are assumed for which relay still detects fault and at the same time makes no reaction for the fault conditions during a single change of a setting step.

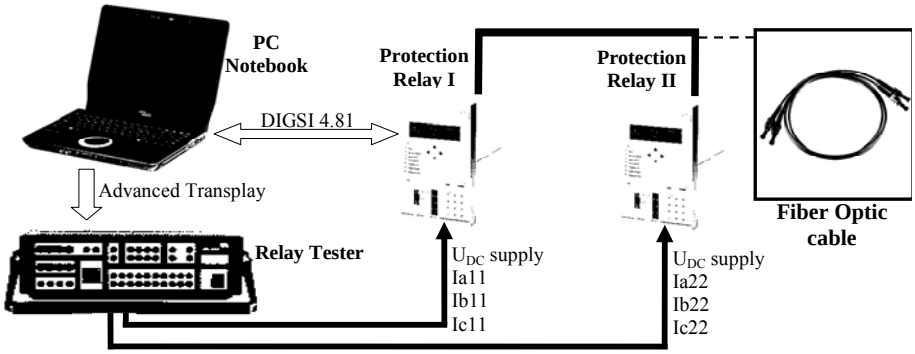

Fig. 9 Experimental test setup.

Table 6 Validation results of operating speed for EMTDC/PSCAD relay model.

Case description	Time interval (ms)	
	Experimental results	PSCAD simulation results
Single-phase to ground internal fault in the middle	8	14
Single-phase to ground internal fault at KYV busbar	8	14
Two-phase to ground internal fault at KYV busbar	14 | 14	15 | 15
Three-phase to ground internal fault KYV busbar	18 | 12 | 18	15 | 10 | 15

Table 7 Validation results of sensitivity for EMTDC/PSCAD relay model.

Internal fault resistance (Ω)	Differential phasor $I_{diff>}$ threshold for tripping		Differential phasor $I_{diff>}$ threshold for non-tripping	
	Experimental results	PSCAD simulation results	Experimental Results	PSCAD Simulation Results
55	4.02	4.05	4.03	4.06
70	3.23	3.25	3.24	3.26
145	1.72	1.73	1.73	1.74
210	1.31	1.32	1.32	1.33

6. Conclusions

EMTDC/PSCAD relay computer model proves to be reliable and efficient from taken simulation cases with established parameter set. Apart from internal and external fault states, analyzed simulation cases included transmission cable's energization and shunt reactor's energization states, giving overall 10 different study cases [8]. All simulation results have been successfully compliant with the expected ones.

According to simulation results, relay model is able to accurately detect internal faults and differentiate them with mentioned other states that may be misleading. Furthermore, relay is able to detect highly-resistive internal faults, which proves high accuracy and sensitivity of the implemented algorithm used for the measurement and comparison of the obtained signals.

Acknowledgments

The first author gratefully acknowledges research support from the Danish TSO-Energinet.dk, which delivered all necessary technical data of the analyzed system along with Siemens SIPROTEC 4 7SD522 relays.

References

[1] T.S. Sidhu, M.A. Hfuda, M.S. Sachdev, Generating relay models for protection studies, IEEE Computer Applications in Power 11 (4) (1998) 3-38.

[2] P. McLaren, K. Mustaphi, G. Benmouyal, S. Chano, A. Girgis, C. Henville, et al., Software models for relays, IEEE Trans. on Power Delivery 16 (2) (2001) 238-245.

[3] L. Wu, C. Liu, C. Chen, Modeling and testing of a digital distance relay using MATLAB/SIMULINK, in: Proceedings of the 37th Annual North American Power Symposium, Oct. 23-25, 2005, pp. 253-259.

[4] S.G.A. Perez, M.S. Sachdev, T.S. Sidhu, Modeling relays for use in power system protection studies, in: Canadian

Conf. on Electrical and Computer Engineering, May 2005, pp. 566-569.

[5] M. Kezunović, User-friendly, open-system software for teaching protective relaying application and design concepts, IEEE Trans. on Power Systems 18 (3) (2003) 986-992.

[6] Applications of PSCAD/EMTDC Application Guide, Manitoba HVDC Research Centre Inc., Winnipeg, Canada, 2008.

[7] G. Ziegler, Numerical Differential Protection: Principles and Applications, Publicis Corporate Publishing, Erlangen, Germany, July 2005.

[8] M. Sztykiel, Protection philosophies for HVAC transmission network, M.Sc. Thesis, Aalborg Univ., Aalborg, Denmark, 2009.

[9] T. Sezi, O. Lippert, A. Struecker, Field Experience Summary with a Line Differential Relay Using Complex Communication Infrastructure, Siemens Energy, Inc., Nuremberg, Germany, Sept. 2009.

[10] J.R. Lucas, Representation of Magnetisation Curves over a Wide Region Using a Non-Integer Power Series, Vol. 25, Manchester Univ. Press, Oct. 1988, pp. 335-340,